

Simulation of Effect of Current Stressing on Reliability of Solder Joints with Cu-Pillar Bumps

Y. Li, Q. S. Zhang, H. Z. Huang, and B. Y. Wu

Abstract—The mechanism behind the electromigration and thermomigration failure in flip-chip solder joints with Cu-pillar bumps was investigated in this paper through using finite element method. Hot spot and the current crowding occurs in the upper corner of copper column instead of solders of the common solder ball. The simulation results show that the change in thermal gradient is noticeable, which might greatly affect the reliability of solder joints with Cu-pillar bumps under current stressing. When the average applied current density is increased from 1×10^4 A/cm² to 3×10^4 A/cm² in solders, the thermal gradient would increase from 74 K/cm to 901 K/cm at an ambient temperature of 25°C. The force from thermal gradient of 901 K/cm can nearly induce thermomigration by itself. With the increase in applied current, the thermal gradient is growing. It is proposed that thermomigration likely causes a serious reliability issue for Cu column based interconnects.

Keywords—Simulation, Cu-pillar bumps, Electromigration, Thermomigration.

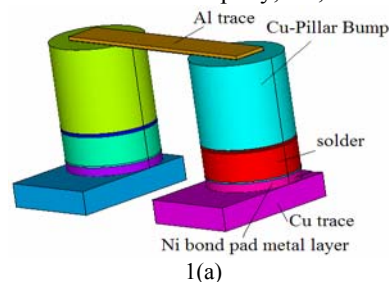
I. INTRODUCTION

WITH the development of microelectronic industry, wire bonding is being replaced by flip-chip technology in wafer-level packaging [1]. Actually flip-chip technology has become a dominating packaging solution for high performance chips and will remain so in the foreseeable future. At present, solder ball interconnection is a common flip-chip assembly scheme in which the solder ball is around 150 μ m to 300 μ m in diameter. With the device size reduced, an increase in device electrical current density and thermal energy density becomes inevitable. A very common mode of electromigration (EM) induced failure in solder joints is the consumption of under bump metallization (UBM) and interfacial void formation because of current crowding at the cathode contact interface between the solder bump and the interconnect line [2]. In order to mitigate this problem, a new flip-chip interconnection with Cu-pillar bumps is introduced, which are around 50 μ m to 100 μ m in diameter, having a thick copper column and a thin solder

tip. Cu-pillar bump has superior electrical and thermal characteristics over the conventional solder ball. Also, it could take form to flexible shapes to effectively resolve the problems associated with solder ball, which are concomitant with the increase in electrical current density and thermal energy density. However, under a high density current, the EM and thermomigration (TM) still may become serious threats to the reliability of Cu-pillar bumps. In this work, by using finite element method the distribution of temperature and current density in Cu-pillar bumps were simulated when the currents of 0.2 A, 0.4 A, and 0.6 A are applied at a constant ambient temperature of 25°C. The corresponding current density ranges from 1×10^4 A/cm² to 3×10^4 A/cm² in bumps. The calculation results can reveal the spots with the most danger of functioning failure, and find out whether the thermal gradient could induce TM.

II. EXPERIMENT

Fig. 1 is a schematic diagram of Cu-pillar flip-chip assembly used for modelling. The dimension of Si chip is 0.25 mm \times 0.1 mm with a thickness of 290 μ m. On the chip side, aluminum trace is 20 μ m wide and 2 μ m thick. The metallization on aluminum trace is a layer of 0.4 μ m thick Ni(V) coating. The diameter of metallization and passivation opening is 50 μ m and 20 μ m, respectively. The Ni(V) is not considered in this model since it is too thin. Copper columns with a height of 50 μ m and a diameter of 50 μ m are electroplated on the Ni(V) layer. On top of them, a layer of 20 μ m thick eutectic tin-lead solder is electroplated as bonding material. The bumps are joined onto Au/Ni(P)/Cu pads of bismaleimide triazine (BT) substrate. The thin layer of gold is not created in this model since it is dissolved into the solder fast during assembly. On the substrate side, the thickness of electroless Ni(P) layer and copper pad is 5 μ m and 14 μ m, respectively. The copper trace acts as pad base material with a width of 50 μ m. The dimension of BT substrate is 2.5 mm \times 2.5 mm with a thickness of 480 μ m. After assembly, the joint pitch is 100 μ m. After assembly, the gap between the chip and substrate is filled with epoxy, i.e., underfill.

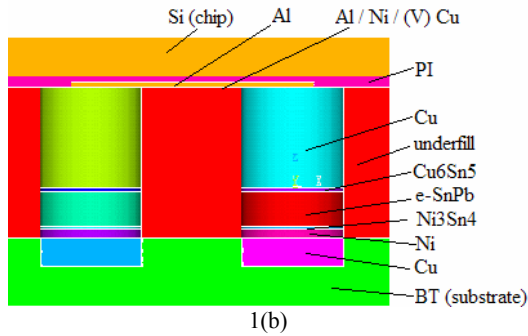


Y. Li is with School of Mechatronics Engineering, University of Electronic Science and Technology of China, Chengdu, Sichuan 611731, China (e-mail: yuanhang555@163.com).

Q. S. Zhang is with School of Mechatronics Engineering, University of Electronic Science and Technology of China, Chengdu, Sichuan 611731, China (e-mail: qiushuzhang@uestc.edu.cn).

H. Z. Huang is with School of Mechatronics Engineering, University of Electronic Science and Technology of China, Chengdu, Sichuan 611731, China (e-mail: hzhuang@uestc.edu.cn).

B. Y. Wu is with School of Mechatronics Engineering, University of Electronic Science and Technology of China, Chengdu, Sichuan 611731, China (e-mail: bywuee@gmail.com).



1(b)

Fig. 1 Schematic diagram of Cu-pillar flip-chip assembly: 1(a) 3D model. 1(b) A cross-sectional drawing of constructing details of model for electrical-thermal coupled simulation

The values of relevant physical properties of materials involved in this simulation are presented in Table I [3], [4]. To display the distribution of current density and temperature during current stressing, a 3D electrothermal coupled modelling was applied to the Cu-pillar interconnection with identical configuration as described above at different currents. The commercial software package ANSYS was employed to carry out model calculations. A solid69 element and a solid70 were used for the electrothermal modelling. In the simulation, the currents of 0.6 A, 0.4 A, and 0.2 A were applied to the pillar. The average current densities at the interface (50 μm in diameter) between copper column and solder were therefore calculated to be $3 \times 10^4 \text{ A/cm}^2$, $2 \times 10^4 \text{ A/cm}^2$, and $1 \times 10^4 \text{ A/cm}^2$, respectively. The bottom of BT substrate had a constant temperature of 25°C. And the value of convection coefficient was set to be 10 $\text{W/m}^2 \cdot \text{C}$ at 25°C [5].

TABLE I
 PHYSICAL PROPERTIES OF MATERIALS FOR MODELLING

Materials	Thermal conductivity (W/m·K)	Resistivity (m Ω .cm)	Temperature coefficient of resistivity (K $^{-1}$)
Al	238.00	2.70	4.2×10^{-3}
Al/Ni(V)Cu	166.60	29.54	5.6×10^{-3}
Cu	403.00	1.70	4.3×10^{-3}
Cu ₆ Sn ₅	34.10	17.50	4.5×10^{-3}
e-SnPb	50.00	14.60	4.4×10^{-3}
Ni ₃ Sn ₄	19.60	28.50	5.5×10^{-3}
Ni	76.00	6.80	6.8×10^{-3}
Si	147.00		
BT	0.70		
Underfill	0.55		
PI	0.34		

III. RESULTS AND DISCUSSION

A. Effect of TM on the reliability of solder joints with Cu-pillar bumps

Most proposed mechanisms behind the failure of solder joints deal with complex forces which drive atoms from one site to another site. Under current stressing, there are at least two types of forces which could give rise to the mass transport of atom.

One is the combined forces of electric field and charge carriers. Another comes from the thermal gradient which may induce TM. Current stressing would cause Joule heating. In a typical flip-chip module, the cross section area of the metal trace on silicon dies is much smaller than that of the solder joint. Thus, the primary heat source is the metal trace that contributes to the most of the electric resistance of the module. Since various materials in the IC package have different thermal properties, the temperature distribution is uneven. The silicon side is relatively hot [6]. The Joule heating resulting from current stressing may produce a thermal gradient in the solder joint. The simulation results for temperature distribution in solder joints with Cu-pillar bumps is shown in Fig. 2. A hot spot exists near the entrance point of the aluminum trace to copper pillar. When the applied current changes from 0.2 A to 0.6 A, the maximum temperature of solder increases substantially from 32°C to as high as 110°C as a result of Joule heating effect. However, the average current density only increases from $1 \times 10^4 \text{ A/cm}^2$ to $3 \times 10^4 \text{ A/cm}^2$, which is smaller as compared with the change in the current density in the solder ball due to the current crowding [7]. Fig. 3 shows the simulation results of thermal gradient distribution in the solder

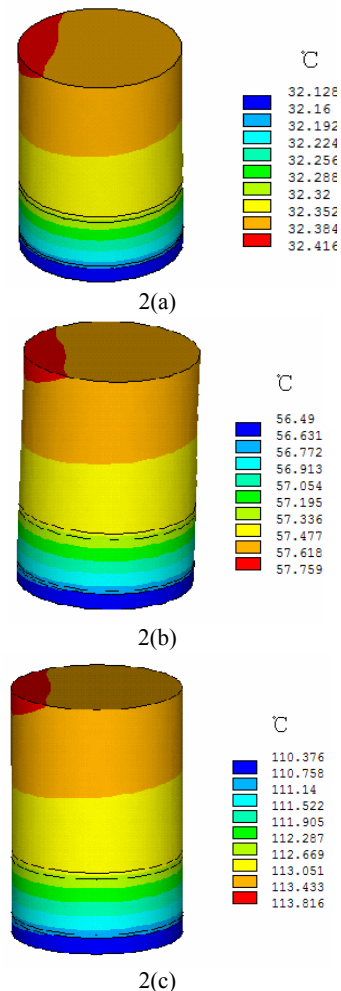


Fig. 2 Temperature distribution in copper pillar bumps with a height of 50 μm and a diameter of 50 μm and solders with 20 μm thickness under different currents: 2(a) 0.2 A, 2(b) 0.4 A, 2(c) 0.6 A.

bumps. The maximum thermal gradient is around 74 K/cm, 329 K/cm, and 901 K/cm at 0.2 A, 0.4 A, and 0.6 A, respectively. The thermal gradient in Cu column bumps is much smaller than it in solder bumps. The study emphasis is therefore put on the thermal gradient in solder bumps.

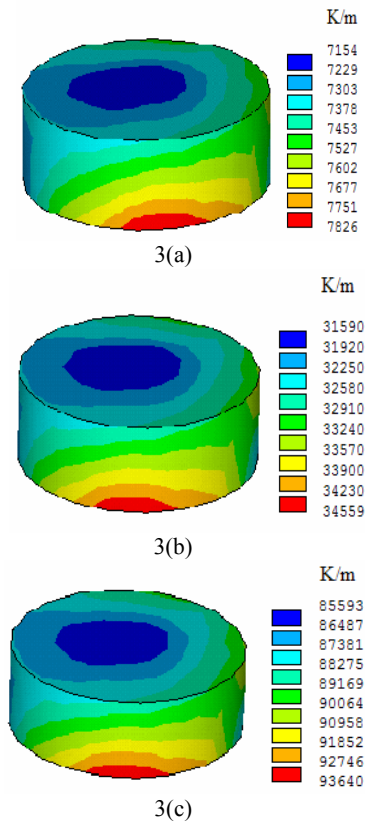


Fig. 3 Thermal gradient distribution in solders with a height of 20 μm and a diameter of 50 μm under different currents: 3(a) 0.2 A, 3(b) 0.4 A, 3(c) 0.6 A.

The thermal gradient might have a great influence on the solder joint failure since it increases quickly with the current. The force from thermal gradient originates from the applied current. It could enhance or weaken the failure. If the hot side is at the anode, the drive force would be weakened and vice versa. The flux equation in TM is represented as

$$J = \frac{DC}{k_B T} \frac{Q^*}{T} \frac{dT}{dx}, \quad (1)$$

where Q^* is heat of transport, which is the difference between the heat carried by a moving atom per mole and the heat of atoms per mole at the hot end, D is diffusivity, C is concentration, and $k_B T$ is thermal energy [8], [9]. The driving force is described by

$$F_{tm} = -\frac{Q^*}{T} \frac{dT}{dx}. \quad (2)$$

In this simulation, the thermal gradient is 901 K/cm at 0.6 A. Lead is the dominant diffusing species at 110°C. It is assumed that the heat of transport Q^* is temperature-independent, and that the value of Q^* is -25.3 kJ/mole [10]. Thus, the driving force for TM can be calculated as

$$F_{tm} = -\frac{Q^*}{T} \frac{dT}{dx} = -\frac{(-25.3 \times 10^3) / (6.02 \times 10^{23})}{383} \times (901 \times 10^2) = 0.99 \times 10^{-17} \approx 1.0 \times 10^{-17} (N)$$

It was reported that a current density of 10^4 A/cm² could induce EM in solder joints [3], [4], [11], [12]. The driving force in EM is given by

$$F_{em} = -Z^* e \rho j, \quad (3)$$

where Z^* is the effective charge number of EM, e is the electron charge, ρ is the electrical resistivity, and j is the current density. If ρ is taken as 10×10^{-8} Ω.m, Z^* as 10, and e as 1.602×10^{-19} C, the driving force for EM can be determined as

$$F_{em} = -(-10) \times (1.6 \times 10^{-19}) \times (10 \times 10^{-8}) \times (1 \times 10^8) = 1.6 \times 10^{-17} (N)$$

The driving force from the thermal gradient in this simulation is found to be comparable to the driving force that causes EM. Furthermore, the thermal gradient will increase sharply with the current. Therefore, TM resulting from the thermal gradient due to Joule heating effect would become an important failure mode in solder joints under current stressing.

B. Effect of EM on the reliability of solder joints with Cu-pillar bumps

Fig. 4 demonstrates the simulation results for current density distribution in thick copper columns and the solder joints under the stressing current. It is observed that current crowding occurs in the upper corner of copper columns, which spreads about 4 μm wide and 8 μm deep into the copper column. The maximum current densities in the whole structure are 2.64×10^5 A/cm², 5.24×10^5 A/cm², and 7.76×10^5 A/cm² at 0.2 A, 0.4 A, and 0.6 A, respectively. The maximum current densities in the solder are 1.25×10^4 A/cm², 2.50×10^4 A/cm², and 3.75×10^4 A/cm² at 0.2 A, 0.4A, and 0.6 A respectively, which are much lower than those in the whole of the structure. However, EM will not happen in the bulk of copper pillar because the current density of 7.76×10^5 A/cm² at 110 °C is not large enough to cause failure in copper. In this Cu-pillar bump, the current crowding occurs in the thick copper instead of the solder in conventional solder ball interconnection. Therefore, this structure of copper columns combined with thin solder bumps could avoid the EM -induced failure, which could take place in

conventional flip chip structures with voids formed at the solder interface due to current crowding.

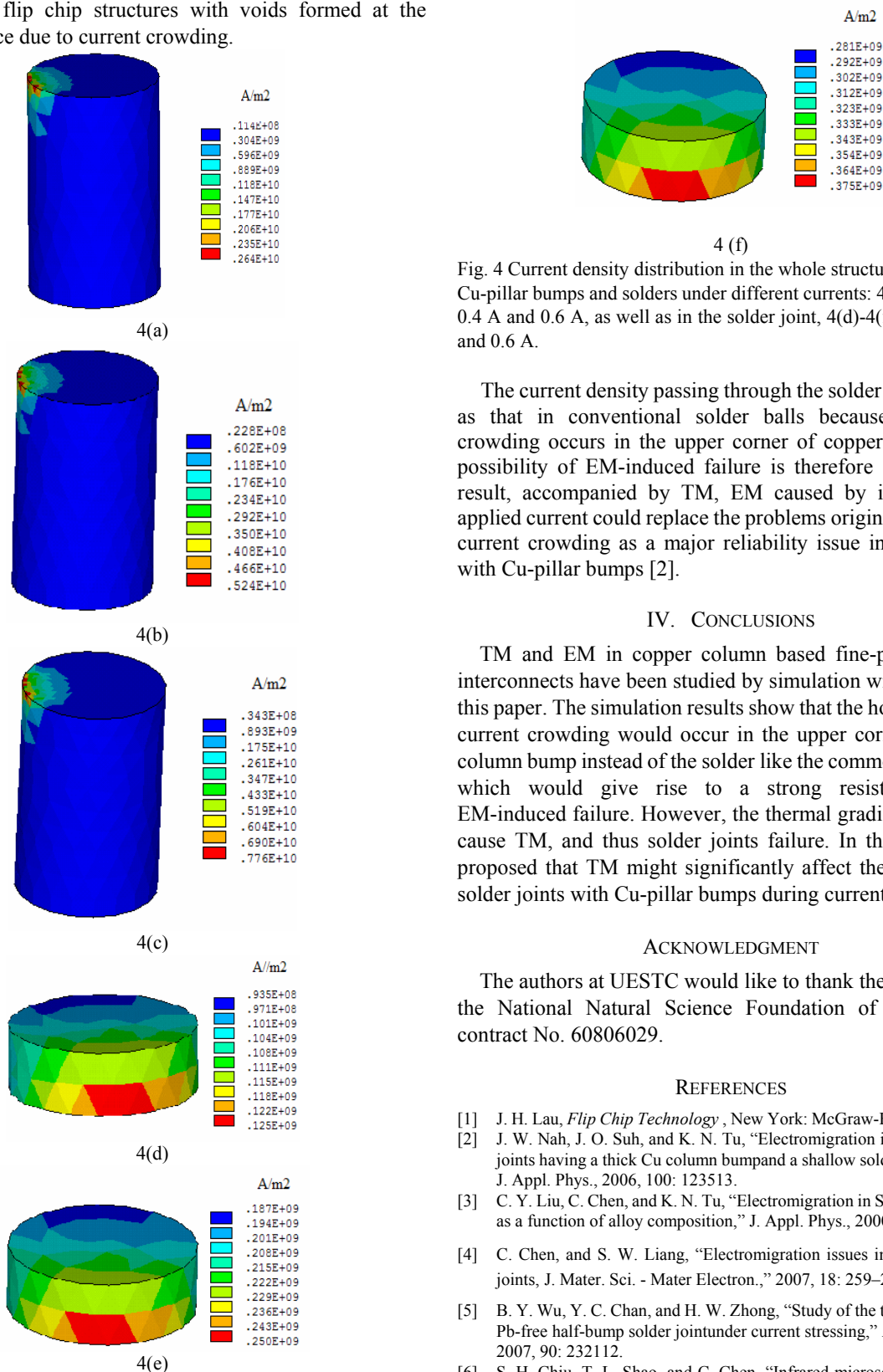


Fig. 4 Current density distribution in the whole structure consisting of Cu-pillar bumps and solders under different currents: 4(a)-4(c): 0.2 A, 0.4 A and 0.6 A, as well as in the solder joint, 4(d)-4(f): 0.2 A, 0.4 A and 0.6 A.

The current density passing through the solder is not as large as that in conventional solder balls because the current crowding occurs in the upper corner of copper column. The possibility of EM-induced failure is therefore smaller. As a result, accompanied by TM, EM caused by increasing the applied current could replace the problems originating from the current crowding as a major reliability issue in solder joints with Cu-pillar bumps [2].

IV. CONCLUSIONS

TM and EM in copper column based fine-pitch flip-chip interconnects have been studied by simulation with ANSYS in this paper. The simulation results show that the hot spot and the current crowding would occur in the upper corner of copper column bump instead of the solder like the common solder ball, which would give rise to a strong resistance against EM-induced failure. However, the thermal gradient will likely cause TM, and thus solder joints failure. In this paper, it is proposed that TM might significantly affect the reliability of solder joints with Cu-pillar bumps during current stressing.

ACKNOWLEDGMENT

The authors at UESTC would like to thank the support from the National Natural Science Foundation of China under contract No. 60806029.

REFERENCES

- [1] J. H. Lau, *Flip Chip Technology*, New York: McGraw-Hill, 1995, pp. 28.
- [2] J. W. Nah, J. O. Suh, and K. N. Tu, "Electromigration in flip chip solder joints having a thick Cu column bump and a shallow solder interconnect," *J. Appl. Phys.*, 2006, 100: 123513.
- [3] C. Y. Liu, C. Chen, and K. N. Tu, "Electromigration in Sn-Pb solder strips as a function of alloy composition," *J. Appl. Phys.*, 2000, 88: 5703.
- [4] C. Chen, and S. W. Liang, "Electromigration issues in lead-free solder joints, *J. Mater. Sci. - Mater Electron.*," 2007, 18: 259-268.
- [5] B. Y. Wu, Y. C. Chan, and H. W. Zhong, "Study of the thermal stress in a Pb-free half-bump solder joint under current stressing," *Appl. Phys. Lett.*, 2007, 90: 232112.
- [6] S. H. Chiu, T. L. Shao, and C. Chen, "Infrared microscopy of hot spots induced by Joule heating in flip-chip SnAg solder joints under accelerated electromigration", *Appl. Phys. Lett.*, 2006, 88: 022110.
- [7] S.W. Liang, T. L. Shao, C. Chen, E. C. C. Yeh, and K. N. Tu, "Relieving current crowding effect in flip-chip solder joints during current stressing," *J. Mater. Res.*, 2006, 21(1): 137-146.

- [8] P. G. Shewmon, *Diffusion in Solids*, Warrendale, PA: TMS, 1989, Chap. 7.
- [9] D. V. Ragone, *Thermodynamics of Materials*, New York: Wiley, 1995, Vol. 2, Chap. 8.
- [10] F. Y. Ouyang, K. N. Tu, Y. S. Lai, and A. M. Gusak, "Effect of entropy production on microstructure change in eutectic SnPb flip chip solder joints by thermigration," *Appl. Phys. Lett.*, 2006, 89: 221906 .
- [11] Y. C. Hsu, T. L. Shao, C. J. Yang, and C. Chen, "Electromigration study in SnAg3.8 Cu0.7 solder joints on Ti/Cr-Cu/Cu under-bump metallization," *J. Electron. Mater.*, 2003, 32: 1222.
- [12] B. Y. Wu, and Y. C. Chan, "Electric current effect on microstructure of ball grid array solder joint," *J. Alloys Compd.* , 2005, 39: 237.